Deterioration of Contemporary Kaihua Handmade Paper: Evolution of Molecular, Supermolecular and Macroscopic Structures

Jingjing Yao (yaojj@fudan.edu.cn)
Fudan University
Ruohong Zhang
Shanghai Institute of Quality Inspection and Technical Research
Chan Luo
Shanghai Institute of Quality Inspection and Technical Research
Yueer Yan
Fudan University
Ning Bi
Shanghai Institute of Quality Inspection and Technical Research
Yi Tang
Fudan University

Research Article

Keywords: Handmade paper, Microstructural evolution, Two-dimensional correlation spectroscopy, Aging and degradation

Posted Date: July 9th, 2021

DOI: https://doi.org/10.21203/rs.3.rs-665580/v1

Abstract

Valued for its toughness and durability, Kaihua paper has been famous in China since the Qing Dynasty and is in the focus of the study on paper life extension. Understanding of the complex degradation behavior of handmade paper under various aging conditions is an essential precondition for preparing contemporary long-life handmade paper. However, reactions sequence and quantitative analysis of microstructure of cellulose and its relation to macroscopic deterioration of handmade paper still are difficult to interpret. Herein, different types of Kaihua handmade papers, produced by various raw materials and crafts, were artificially aged to study the different evolution of their multi-scale structures in dry-heat (DH) and wet-heat (WH) conditions systematically. Two-dimensional correlation spectroscopy (2D-COS) distinguished possible carbonyl vibrations involving hydrolysis and oxidation of cellulose and gave sequential changes of various carbonyl groups, illustrating different evolution behaviors of molecular structure of papers in DH and WH aging process. The energy and distance of hydrogen bond, crystal size and microfiber accessibility were quantitatively calculated during the degradation of cellulose. The dual roles of water molecules, as plasticizers for fibers and as carriers of protons, continuously promoting the hydrolysis of cellulose at molecular and supramolecular scales were elucidated further. In addition, correlations between microstructural evolution and macroscopic deterioration of handmade papers involving reduced mechanical properties and yellowing were revealed.

Introduction

Traditional handmade paper, as an important carrier of inheriting human civilization, is featured excellent performance of its durability (Hubbe and Bowden 2009; Jeong et al. 2014a,b; Luo et al. 2019). It enjoys a great reputation as the king of paper that could last for more than 1000 years (Luo et al. 2021; Tang et al. 2017). Kaihua paper is a kind of legendary handmade paper in China, which was used exclusively by the imperial palace in the Qing Dynasty. It was considered that the craft of Kaihua paper has reached the pinnacle of ancient papermaking, which has great culture value. In recent years, the Research Institute of Kaihua Paper has been established in Kaihua County to restore Kaihua handmade paper, which represents one of the highest levels in China. Although modern papermaking techniques have enhanced the production efficiency, the resultant loss of quality in handmade paper, especially long-term stability, calls for a united effort on this common decline. (Luo et al. 2021; Baty et al. 2010). Hence, it is of fundamental importance to understand the dynamic degradation of paper in multi-scale structures, and find out how an accumulation of microscopic variation of cellulose structure results in the macroscopic deterioration of handmade paper involving discoloration and loss of mechanical resistance, which will enable ultimately access to preparing long-life handmade paper and possessing the great significance to the restoration of ancient books and cultural relics.

Presently, degradation of handmade paper is controlled by mixed hydrolytic and oxidative mechanisms at molecular scale, which is accelerated autocatalytically by protons and active oxygen species. It has been characterized by IR, UV/Vis, Raman and NMR spectroscopic method due to the nondestructive characteristics of these testing methods (Bicchieri et al. 2019; Chiriu et al. 2020; Chiriu et al. 2018;

Corsaro et al. 2016; Fazio et al. 2019; Lojewski et al. 2010; Mallamace et al. 2018; Yonenobu et al. 2009). Carbonyl groups of various degrees of freedom as good candidates, which exhibit high activity in FTIR spectra, are able to trace the changes of molecular structure of cellulose involving mixed hydrolytic and oxidative mechanism (Abidi et al. 2014; Celino et al. 2014; Liu et al. 2017). J. Lojewska defined the oxidation index in FTIR to follow the degradation of cellulose and demonstrated a parallel-consecutive mechanism of cellulose oxidation by fitting the spectra with multiple Gaussian-Lorentzian functions (Lojewska et al. 2005, 2006). However, the band assignment remains unsatisfied since the peaks at rang of 1600 to 1800 cm^{-1} are weak and overlapping. Moreover, the attempt to distinguish the sequence of reactions and their interactions is much more difficult.

Two-dimensional correlation spectroscopy (2D-COS) offers a powerful tool to explore the reaction process at the molecular scale in complex systems and evaluate the differences appearing during an external perturbation. (Hou and Wu 2019a; Moran et al. 2012; Park et al. 2018). This method typically improves the spectral resolution and gives new information, which cannot be obtained in conventional infrared spectra and its derivatives. The cellulose structure has been studied at a variety of perturbations such as the temperature, pressure, concentration and compositions by 2D-COS to investigate the molecular evolution (Hou and Wu 2019b; Yang et al. 2020). J.Zieba Palus et al. also reported that the 2D-COS allowed to differentiate the contribution of paper components including cellulose, carbonates and kaolinite. (Zieba-Palus et al. 2017)

In addition, according to the most recent findings, the supramolecular structure of cellulose, which generally impedes degradation, plays a decisive role in determining the degradation rate and process (Ciolacu et al. 2008; Fazio et al. 2019; Lin et al. 2020; Yang et al. 2019). Several studies have been taken to explore the variation of microstructure of cellulose microfibril, involving crystallinity, crystallite thickness and accessibility in various conditions including hydrothermal, thermo-hygro-mechanical, dry and wet treatment during degradation of cellulose (Hajji et al. 2016; Inagaki et al. 2010; Toba et al. 2013; Xing et al. 2020). A morphological model was proposed by Tesuya Inagaki et al. to describe the difference of the fine structure of the microfibrils in cellulose for hydrothermal and aging degradation. (Inagaki et al. 2010). Teodonio et al. performed the AFM-based nano-mechanical mapping of single cellulose fiber from paper and gave a nanoscale analysis of degradation process (Teodonio et al. 2016). Nevertheless, paper degradation is a complex system, especially for handmade paper with various raw materials and papermaking process. Recent studies offer little information on the dynamic changes of microstructure systematically from molecule to supermolecule for various handmade papers and aging conditions. Furthermore, the relationships between multiscale microstructure and macro properties are still unclear so far.

Herein, we focus on the evolution of the multi-scale structure of four typical handmade papers (with various raw materials and papermaking process produced in Kaihua, China) in DH and WH accelerated aging conditions. 2D-COS analysis has been applied to distinguish carbonyl groups of various degrees of freedom from the hydrolytic and oxidative path and trace their evolution sequence. Moreover, the dynamic changes of multiscale structure for various handmade materials are investigated to offer

quantitative analysis during the aging process systematically in terms of groups, molecular chain, crystal structure, hydrogen bonding networks and microfibril morphology under different external conditions (relative humidity, temperature). In this way, the multi-scale structural evolution of various handmade papers from molecule to supermolecule is traced, which can be associated with the deterioration of macroscopic characteristics, and make a better understanding of various degradation mechanism of handmade papers.

Materials And Methods

Materials

Four types of Kaihua papers (1# Wikstroemia monnula-A, 2# Green wingceltis, 3# Wikstroemia monnula/Green wingceltis (6:4), 4# Wikstroemia monnula-B) were obtained from the Research Institute of Kaihua Paper. Wikstroemia monnula was collected from forests in the mountains near Kaihua county in Quzhou city, Zhejiang province in China. 4# Wikstroemia monnula-B was prepared according to the traditional method through lime (CaO) cooking twice (each 12 hours) and potash (K_2CO_3) bleaching once (15 days). 1#-3# samples made some changes, which were mainly reflected in the cooking process only once: adding sodium carbonate and cooking at 120 ℃ for 8 hours. After cleaning, sodium hypochlorite was added to bleach for 3 hours, and then mechanical pulping was used. The degree of polymerization, morphology and other basic properties of fiber in each paper were given in supporting information (SI.1).

The 2,3,5-triphenyltetrazolium chloride (TTC, ≥ 98.0%) and copper ethylenediamine (1.0 M) were purchased from Sigma Aldrich. Methanol (≥ 99.7%), glucose, potassium hydroxide (KOH, ≥ 98.0%), sodium chloride (NaCl, ≥ 99.8%) and hydrochloric acid (HCl, 36.0–38.0%) used in this work were purchased from Sinopharm Chemical Reagent CO., Ltd.

Accelerated aging of samples

For dry-heat (DH) aging, all samples were placed into a temperature controlled dry-heat oven at 120 ± 2 ℃ for 1, 3, 5, 7, 14, 21, 28, 42, 56 and 70 days. This temperature is chosen in agreement with the conditions of accelerated aging for the cultural durable paper giving by the standards ISO 5630/4-1986 and GB/T 464. For wet-heat (WH) aging, considering more profound changes occurred in higher humidity, all samples were placed into a temperature and relative humidity (RH) controlled oven at 70 ℃ and 80% RH.

Group content measurement

The content of reducing carbonyl group was determined according to the colorimetric method proposed by Szabolcs and Matija (Kocar et al. 2004). The content of carboxylic acid group was measured using conductometric titration methodology (Saito and Isogai 2004). More details can be found in SI.3 from supplementary data.

Crystalline-amorphous structure measurement

The crystallinity, crystal size and spacing were determined by X-ray diffractometer (D8 Advance, Bruker). The incident X-ray radiation was the Cu Kα with a power of 30 kV and 10 mA. The crystalline index, crystal size and d-spacing of samples were calculated through the peak area method (Eq. 1), Scherrer equation (Eq. 2) and Bragg equation (Eq. 3) respectively in SI.4.

Degree of polymerization measurement

Intrinsic viscosities of the samples were obtained by a Nordic viscometer using 0.5 M of copper ethylenediamine as the solvent, and were calculated to degrees of polymerization (DP) by the reported method (De Silva and Byrne 2017).

ATR-FTIR spectroscopy and Two-dimensional correlation spectroscopy (2D-COS) analysis

FTIR spectra were collected using the FTIR spectrometer (Frontier, Perkin Elmer) with a sampling accessory diamond window. All spectra were recorded on ATR mode at 4 cm^{-1} resolution in the region of 600–4000 cm^{-1} and 16 scans. Three points were tested on each sample. For the analysis of carbonyl bands, all papers were placed in the oven at 100℃ for 30 min before experiments to desorb free water whose bending vibrations mask the carbonyl bands. Additionally, collecting the spectra at the oven lamp to prevent the samples from re-absorbing water. 2D-COS analysis was carried out from ART-FTIR spectra as input data for generating correlation maps via 2Dshige software. As for the analysis of hydrogen bond, the DH and WH weathered samples were carefully re-conditioned at 23℃ and 50% RH before measurements. The area of the CH vibration band (2900 cm^{-1}) of the initial spectrum was the normalization factor for absorbance values. The hydrogen bonds peaks were obtained by deconvolution and peak-fitting. The energy and distance of hydrogen bond can be calculated by Eq. 4 and Eq. 5 in SI.5.

Morphology measurement

Scanning electron microscopy (SEM) images were taken by a microscope (FEI FP Quanta 250) at the voltage of 15 kV and a working distance of 7 mm.

Tensile measurement

The tearing strength of the sample was determined by using the falling pendulum (elmendorfs) apparatus (Thwing-albert) according to PN-EN ISO 13937: 2002 test standard. The sample was balanced and measured at 23 ℃ and 50% RH with dimensions of 60 mm length and 60 mm width. The tearing strength test was repeated to get the average value of three specimens.

Color measurement

Color measurements of sample were recorded using a spectrometer (Lorentzen-wetter). Three replicates were measured at three locations on each specimen. The change in color $\triangle E$ was calculated using the

following equation: $\triangle E=\sqrt{\Delta L^2+\Delta a^2+\Delta b^2}$; $\triangle L$, $\triangle a$ and $\triangle b$ are the differences between the initial and final values of L, a and b, respectively (Fabiyi et al. 2008).

Results And Discussion

The experimental objects of this work were four typical handmade papers produced in Kaihua in Zhejiang Province, where the production of Wikstroemia plants accounted for more than 90% in China during the 1960s. Thick bast and thin fiber of Wikstrokea skin meet the requirement of making high-quality handmade paper, leading to the good toughness and excellent durability of some traditional handmade paper such as Dongba paper and Zang paper in China, and Gampi paper in Japan. Kaihua, where might produce imperial paper in Qing Dynasty, has developed a number of excellent traditional handmade papers. Herein, we first carried out the characterization of basic physical and chemical properties in terms of four handmade papers (Table S1 and Fig.S1).

Our work concentrates on the multi-scale analysis of the microstructure evolution and degradation of various Kaihua handmade papers at different aging conditions. The correlation between micro-structure with macroscopic properties is highlighted, whereby the microstructural dependence in terms of molecule and supermolecule is the key issue.

Evolution of molecular structure of Kaihua handmade paper in DH and WH aging process

Regarding the monitoring of cellulose degradation at molecule scale, carbonyl groups with various degrees of freedom can be good candidates to trace the changes in the handmade paper caused by hydrolysis and oxidation reactions (Lojewska et al. 2005; Olsson and Salmen 2004). As shown in Fig. S2, the variation of one-dimensional spectra in the region of 1600–1800 cm^{-1} can be easily visualized during aging process for all samples. However, the most relevant changes in intensities of four typical handmade papers are observed in the region of 1730–1760 cm^{-1} for DH aged papers and 1680–1750 cm^{-1} for WH aged samples, respectively, indicating that different processes occur in DH and WH conditions.

The samples are evaluated through 2D-COS from the time-dependent infrared spectra of the aged handmade papers (Fig. 1). All samples including 1#-4# handmade papers conform to this behavior, illustrating basically similar changes of molecular structure for various raw materials and technics. Taking 1# handmade paper as an example, the regions from 1800 to 1580 cm^{-1} of the 2D-COS, where has proved to follow the degradation of aged cellulose under various conditions, are shown in Fig. 1a-h. Considering the complex reaction stage in aging process and to pick up useful local features of the correlation profiles, we evaluate 2D maps for two treatment time ranges of 0–7 days and 7–70 days.

In the synchronous spectrum of 1# in DH condition (Fig. 1a), important auto-peaks at 1595, 1695, 1715, 1745 cm^{-1} were evidenced. The presence of these peaks is assigned to C = C stretching from lignin, conjugated carbonyl, aldehydic groups and ester from cellulose, respectively, which indicates that these

peaks undergo significant changes. More information can be obtained from the asynchronous correlation spectrum. As shown in Fig. 1b, four positive cross-peaks at 1695–1745 cm^{-1}, 1695–1715 cm^{-1}, 1715–1745 cm^{-1}, 1595–1695 cm^{-1} are observed. According to the Noda's fundamental rule, the following sequence of spectral changes was evidenced: 1595 > 1695 > 1715 > 1745. In the second range of 7–70 days (Fig. 1c and d), changes of peaks at 1735 and 1760 cm^{-1} assigned to carboxylic group (Lojewska et al. 2005) and gamma lactone (Fabiyi et al. 2008) are identified in addition to the peaks at 1595, 1695, 1715, 1745 cm^{-1}. The assignment of bands supports the consecutive character of the reaction mechanism and the band around 1735–1745 cm^{-1} reveals a final oxidation stage of carbon atoms. We finally obtain the following sequence of the spectral change after 7 days: 1745→1735→1715, 1760 cm^{-1}. This order of reaction means that C = C from lignin changes first, followed by conjugated carbonyl, aldehydic groups and ester from cellulose. In the second exposure time range, ester exhibits a profound change and carboxylic acids occur as a final oxidation stage of carbon atoms. We can infer that 1# handmade paper mainly experiences a complex oxidation reaction pattern in DH aging process, starting from ketones turning into conjugated diketones and from aldehydes into carboxylic acid. Simultaneously, intramolecular esterification between acid and alcohol gives rise to lactone.

The spectral region from 1800 to 1580 cm^{-1} of 1# in WH condition, shows some different characteristics of the 2D-correlation IR spectra compared with DH aged samples (Fig. 1e-h). In the synchronous 2D-correlation IR spectrum of WH aging, one broad auto-peak at 1715 is observed throughout the aging process. This auto-peak can be considered to be generated from hydrolysis of hemiacetal bonds and eventually produce aldehyde groups by opening the terminal rings, which is supported by one reaction path that converts carbon atoms from glucopyranose into aldehydic group based on a simple hydrolysis model (Lojewska et al. 2006). Different from dry-heat aging process, the predominant reaction is hydrolysis in the presence of water vapor.

According to the analysis of synchronous and asynchronous spectra, the following sequence of the spectral changes is established: 1595 > 1695 > 1715 > 1735 > 1745 cm^{-1} in the range of 0–7 days and 1715 > 1695 > 1735 > 1745 cm^{-1} in the range of 7–70 days, indicating that modification occurs in C = C from lignin at the beginning of aging, followed by the conjugated carbonyl, aldehydic groups, carboxylic group and ester from cellulose. For longer treatment time, an increase of the extent of modification of aldehydic groups continues to taking place and prior to carboxylic group and ester.

Therefore, the moment of absorbed water and C = C bonds of substituted aromatic ring coupled with conjugated C-O bonds in lignin is changing first, followed by carbohydrates. Although the oxidation and hydrolysis reactions occur in both DH and WH aging process, different behaviors are showed, especially after 7 aging days. The increase of carbonyl and carboxyl groups in the first seven days proves that oxidation and hydrolysis occur simultaneously. The water molecules accelerate the production of carboxyl groups, which further promote the occurrence of hydrolysis. As the aging time increases, the content of carboxyl group increases rapidly in DH condition because of a series of consecutive oxidative reactions (Fig. S3a and b). While the content of aldehyde increases rapidly in WH condition, indicating

that hydrolysis process still plays a main role and generates the mainly formation of aldehydic groups on terminal rings (Fig. S3c and d).

We further verified the aging process under different conditions through the changes of breakage rate of cellulose molecular chain and integral area dynamics curve from infrared spectrum. The increase in number of chain scissions is the essential mechanism of cellulose degradation. As shown in Fig. 2a, the number of molecular chain breaks show a different trend in DH and WH condition. In WH condition, the function fits well to the data and the kinetic curve is closed to 1st order rate law, indicating the predominating reaction is hydrolysis, which is in accordance with the Ekenstam model. In DH condition, an important feature of curve is that it exhibits acceleration followed by chain breakage number stabilization. The kinetic curve in DH seems complicated and a single exponential function does not fit it, reflecting a complex reaction. All this information can be consistent with our previous two-dimensional infrared analysis results. Oxidation and hydrolysis occur in the initial stage in DH. After seven days, oxidation predominates and precedes hydrolysis. The main reaction is hydrolysis in WH condition and water molecules catalyze the hydrolysis of glycosidic bonds.

As mentioned above from 2D-COS, the carbonyl groups with different degrees of freedom at the region of 1640 ~ 1800 cm^{-1} in FTIR reveal a good ability to trace the hydrolysis and oxidation of handmade paper. Therefore, we build a model to reflect the aging process of various handmade papers based on the change of the integral area from 1680–1800 cm^{-1} in the normalized infrared spectrum. The integral quantization of carbonyl bands in infrared spectra has been proved to be feasible (Lojewska et al. 2005). In this work, we narrowed the integral region and concentrated on the more sensitive parts. As shown in Fig. 2b, the integral area kinetic curve is similar to the kinetic curves based on DP measurements, except that the gap between DH and WH is reduced after 7 days. This shows that the infrared spectrum reflects well on the occurrence of oxidation reactions in this region. The mixing mechanism of hydrolysis and oxidation of handmade paper is effectively represented during the aging process, which indicates the feasibility of non-destructive monitoring of aging behavior via infrared spectroscopy. We calculate the exact content of reducing carbonyl and carboxyl by colorimetry and titration methodology, respectively. The total amount of them is in accordance with the curve of infrared integration, which further confirms the reasonableness of the aging process that we inferred (Fig. 2c).

Evolution of supramolecular structure of Kaihua handmade paper in DH and WH aging process

The supramolecular structure of cellulose plays a crucial role in determining the rate of degradation process, as a high supramolecular order of the polymer chain usually impedes degradation. We carry out an analysis of ultra-structure to illustrate evolution of the hydrogen bond and crystalline-amorphous region in greater detail using peak fitting method.

We trace the change of hydrogen bond for 1# sample by FTIR and calculate the energy and distance of hydrogen bond. As shown in Fig. 3a and b, the intramolecular hydrogen bonds for O (2)H…O (6) and O (3)H…O (5) and the intermolecular hydrogen bonds for O (6)H…O (3') of cellulose I are observed at 3440–

3480 cm^{-1}, 3300–3330 cm^{-1} and 3140–3180 cm^{-1}, respectively. The result shows that the effect of the aging process on the hydrogen bond is limited until 70 days. However, some differences still can be observed between DH and WH aging process. For dry-heat accelerated aging, the energy of all hydrogen bonds first increases and then decreases with the prolonging of aging time. Among them, the O (2) H…O (6) bond has the lowest hydrogen bond energy, which can be easily changed. The initial hydrogen bond energy of 1# for O (2)H…O (6), O (3)H…O (5) and O (6)H…O (3') is 13.73, 23.96 and 34.63 kJ/mol, which increases by 4.1%, 1.5 and 1.2% after 28 days, and then decreases by 2.4%, 1.0% and 0.7% after 70 days. For WH aging, the intermolecular hydrogen bond energy of O (6)H…O (3') shows slightly reduced energy and increased distance, while the intramolecular hydrogen bond only exhibits mild fluctuations.

On the other hand, we explore the effect of various aging conditions on crystalline-amorphous structure by XRD. In Fig. 3c, all handmade papers exhibit cellulose I since typical diffraction peaks at 14.48–4.98, 16.1-17.89 and 22.2–23.0 can be observed, which are ascribable to the (1–10), (110) and (200) crystallographic planes of cellulose I, respectively. The lattice constants of four handmade papers remain basically unchanged and no distortion occurs after accelerated aging for 70 days. We obtain the crystallinity, crystal size and interplanar spacing via SI.4. As shown in Fig. 3c and d, no significant change of crystallinity in aging process is observed even after 70 days, suggesting that most of the aging degradation takes place in the amorphous zone. The crystal size in DH aging process does not change too much, while crystal size gradually increases in the early stage of WH aging and then becomes constant in the latter stage. It is also found that interplanar crystal spacing gradually increased with the process of aging both in DH or WH condition, indicating that the accessibility is increased due to the molecular chain breaking and more loose structure in amorphous region.

Those results reflect that the degradation mainly occurs in the amorphous zone, and decreased DP also causes slight imperfections in the crystalline structure, which is more obvious in the system with water vapor. Based on the evolution of molecular and supramolecular structures, we propose a mechanism diagram to illustrate the difference of the fine structure of paper cellulose in DH and WH aging process (Fig. 3e). In DH condition, the removal of bond water contributes to the increase of hydrogen bond energy, causing free hydroxyl group on the cellulose chain to recombine and form new intramolecular and intermolecular hydrogen bonds, which results in the increase of hydrogen bond forces and the decrease of hydrogen bond spacing. Hydrolysis and oxidation reactions occur after dehydrated, which cause the breaking of molecular chains and retard continuous formation of intermolecular hydrogen bond. Therefore, the loss of bond water is an important reason that accelerates aging process. In WH condition, water molecules enter the amorphous regions and react with different cellulose-surface hydroxyl groups. A fraction of intermolecular hydrogen bonds of cellulose chains is lost and compensated by hydrogen bonds with water molecules. As a result, the cellulose chain structure is slightly loose, leading to the decreased energy and increased distance of intermolecular hydrogen bond (Wang et al. 2014). At a same time, a swelling of the cellulose chain structure generates a release of some strain that is originally in place in the cellulose chains, leading to few imperfections, expanded d-spacing and increased accessibility between microfibers in crystalline region. Therefore, long-term effects of water have much

more harmful to handmade paper due to water molecules as a dual function: as a plasticizer for cellulose and as carriers of protons, catalyzing the hydrolysis of hemiacetal bonds.

These two different processes can also be verified on SEM images in Fig. 4. As for the DH aging, the fibers of Wikstroemia monnula fiber (1#) begin to be slightly tapered and peeled after 7 days. As the aging time further increases, reduced diameter and peeling can be observed resulting from dehydration and broken bonds. Different from DH aging, the fibers show obvious swelling behavior during WH aging process. The fiber starts to appear flake and organize into bundles of aligned fibers once the aging reaction occurs. The longer the aging days are, the higher the fibers swell. This swelling behavior is probably linked to the infiltration of water molecular in handmade paper matrix.

The effect of craft and raw materials on aging degradation of Kaihua handmade paper

Furthermore, the effects of craft and raw materials on aging degradation of handmade paper are studied. As shown in the Fig. 5a, the rate of chain scission increases as a two stages model, similar to infrared integral area curve in Fig. 5b. Specifically, the degradation rates of 1# to 4# handmade papers in early stages are 6.97×10^{-5}, 9.63×10^{-5}, 6.34×10^{-5}, 4.91×10^{-5} in DH and 6.95×10^{-5}, 5.81×10^{-5}, 2.48×10^{-5}, 1.48×10^{-5} in WH respectively, exhibiting that degradation seriously depends on the cooking and bleaching process: the chain scission rate of 4# handmade paper with traditional CaO cooking and plant ash bleaching process is approximate five times lower than that of the Na_2CO_3 cooking and sodium hypochlorite bleaching process (1#) in WH. In addition, the aging rate of handmade paper with hybrid materials is lower than that of single wikstromia and green sandalwood.

Since the dominance of amorphous degradation and very slow degradation in the crystallization zone, an equilibrium is reached when the fast consumption of the glycosidic bonds in the amorphous region. Combined with the changes of DP, crystal structure and hydrogen bond of four handmade papers during degradation, we found that the aging process is relevant to the initial amount of glycosidic bonds and stability of weak link in the amorphous regions, and is also affected by the changes of pH level. Although the raw material and initial crystallinity of 4# handmade paper is similar to that of 1#, 4# handmade paper remains more glycosidic bonds in the amorphous region by traditional processing, making the chain breaking rate slow down (Fig. S4 and Fig. S5). As shown in Table S2, 4# handmade paper also shows a more stable hydrogen bond network involving energy and accessibility under all conditions. Moreover, we note that the SEM-EDS analysis indicates that 4# paper contains micron-sized particles with a high level of calcium that are spread in the handmade paper, which could be a product of the traditional pulp technology (Fig. 5d). Although other types of handmade papers contain calcium content, their content is much lower than that of 4#. Those micro-sized and calcium-rich particles in 4# handmade paper, presumably calcium oxide or calcium hydroxide, are effective in neutralizing acidic products of the hydrolysis of paper. The slowest rate of pH change of 4# handmade paper in four handmade papers proves it (Fig. 5c).

Relationship between macroscopic degradation and microstructural change

These microscopic changes that we have discussed ultimately affect macroscopic performance. Finally, we test the chromatic aberration and tearing degree of handmade paper with various aging conditions.

As shown in Fig. 6a and b, the tearing strength resistance of four handmade papers decreases by 36.5–47.9% in DH condition and by 37.2–49.6 % in WH condition after 70 days. The trend of tearing strength resistance (Fig. 6a and b) is highly consistent with that of the degree of polymerization (Fig. 5a). The decline rate of the first stage ranks as: 1#>2#>3#>4#, indicating that the decline rate of mechanical properties of handmade paper is positively related to the molecular chain breaking rate of handmade papers. Interestingly, the results show that the formation of chromatic aberration has little to do with the amount of lignin, but strongly depends on the number of carbonyl groups in the form of aldehydes and conjugated diketones. The initial carbonyl content determines the rate of chromatic aberration, and the final chromatic aberration value is positively correlated with the carbonyl content generated during aging process (Fig. 6c-f). The bleaching method of hypochlorite acid introduced more ketone groups and aldehyde groups, so the handmade paper (1#-3#) prepared by this process has more initial carbonyl group content and a higher yellowing rate than the handmade paper (4#) prepared by the traditional process. Kyujin Ahn et al reported that the carboxyl group did not give rise to chromophore generation independent whether present as a free acid or in their protected form of a lactone. However, the carboxyl group promotes and degenerates the color condensation reaction of carbonyl groups (Ahn et al. 2019). This can explain that 4# handmade paper still shows the slowest coloration rate due to its lower carbonyl content, although with higher lignin and carboxyl content. Also, the WH aging process appears more pronounced yellowing compared with DH aging, which because the continuous generation of new reductive terminal carbonyl groups are produced from hydrolysis when water molecules are present, making the chromatic aberration value increases rapidly.

Conclusions

In summary, a systematic study of multi-scale structure evolution of four typical Kaihua handmade papers in DH and WH accelerated aging process is reported. The different degradation mechanism of Kaihua handmade paper in DH and WH aging process is revealed. 2D-COS distinguishes possible carbonyl vibrations involving hydrolysis and oxidation of cellulose and gives different reaction paths of molecular structure of paper in DH and WH conditions. The energy and distance of hydrogen bond, crystal size and microfiber accessibility are quantitatively calculated during the degradation of cellulose. A dual function of water molecules is further recognized: as a plasticizer for fiber and as carriers of protons, continuously promoting the hydrolysis of cellulose and will be more harmful to the lifetime of handmade paper in the long run. The degradation behavior of different types of papers also indicates that the handmade paper produced by traditional craft exhibits more excellent durability due to the more initial glycosidic bonds, relatively stable hydrogen bond networks and higher pH value in it.

In addition, correlations between microstructure evolution and macroscopic deterioration of paper are explained. The yellowing of handmade paper is determined by the content of aldehydes and conjugated diketones carbonyl groups, while the decreasing rate of mechanical properties is positively correlated with

the fracturing rate of molecular chain of handmade paper. All the information helps to elaborate the complex degradation mechanism of handmade paper under different aging conditions, and will be the startup for the design of more durable handmade paper.

Declarations

Acknowledgements

This work was supported by China Postdoctoral Science Foundation (2021M692149), National Natural Science Foundation of China (21805042), Shanghai Pujiang Program (2020PJC003), Shanghai Sailing Program (18YF1401400), Program of Shanghai Institute of Quality Inspection and Technical Research (KY-2020-1-QH) and Public Service Platform of Shanghai Science and Technology Commission (14DZ2293000).

Conflict of interest

The authors declare that they have no conflict of interest.

Ethical approval

This article does not contain any studies with animals or human participants performed by any of the authors. The authors claim the compliance with the ethical standards.

References

1. Abidi N, Cabrales L, Haigler C H (2014) Changes in the cell wall and cellulose content of developing cotton fibers investigated by FTIR spectroscopy. Carbohydrate Polymers 100: 9-16.
2. Ahn K, Zaccaron S, Zwirchmayr N S, Hettegger H, Hofinger A, Bacher M, Rosenau T (2019) Yellowing and brightness reversion of celluloses: CO or COOH, who is the culprit? Cellulose 26(1): 429-444.
3. Baty J W, Maitland C L, Minter W, Hubbe M A, Jordan-Mowery S K (2010) Deacidification for the conservation and preservation of paper-based works: a review. BioResources 5(3): 1955-2023.
4. Celino A, Goncalves O, Jacqu emin F, Freour S (2014) Qualitative and quantitative assessment of water sorption in natural fibres using ATR-FTIR spectroscopy. Carbohydrate Polymers 101: 163-170.
5. Chiriu D, Pisu F A, Ricci P C, Carbonaro C M (2020) Application of Raman spectroscopy to ancient materials: models and results from archaeometric analyses. Materials 13(11): 2456.
6. Chiriu D, Ricci P C, Cappellini G, Salis M, Loddo G, Carbonaro C M (2018) Ageing of ancient paper: a kinetic model of cellulose degradation from Raman spectra. Journal of Raman Spectroscopy 49(11): 1802-1811.
7. Ciolacu D, Ciolacu F, Popa V I (2008) Supramolecular Structure - A Key Parameter for Cellulose Biodegradation. Macromolecular Symposia 272: 136-142.

8. Corsaro C, Mallamace D, Vasi S, Pietronero L, Mallamace F, Missori M (2016) The role of water in the degradation process of paper using 1H HR-MAS NMR spectroscopy. Physical Chemistry Chemical Physics 18(48): 33335-33343.
9. De Silva R, Byrne N (2017) Utilization of cotton waste for regenerated cellulose fibres: influence of degree of polymerization on mechanical properties. Carbohydrate Polymers 174: 89-94.
10. Fabiyi J S, McDonald A G, Wolcott M P, Griffiths P R (2008) Wood plastic composites weathering: visual appearance and chemical changes. Polymer Degradation and Stability 93(8): 1405-1414.
11. Fazio E, Corsaro C, Mallamace D (2019) Paper aging and degradation monitoring by the non-destructive two-dimensional micro-Raman mapping. Spectrochimica acta. Part A, Molecular and biomolecular spectroscopy 228: 117660-117660.
12. Hajji L, Boukir A, Assouik J, Pessanha S, Figueirinhas J L, Carvalho M L (2016) Artificial aging paper to assess long-term effects of conservative treatment. Monitoring by infrared spectroscopy (ATR-FTIR), X-ray diffraction (XRD), and energy dispersive X-ray fluorescence (EDXRF). Microchemical Journal 124: 646-656.
13. Hou L, Wu P (2019a) Exploring the hydrogen-bond structures in sodium alginate through two-dimensional correlation infrared spectroscopy. Carbohydrate Polymers 205: 420-426.
14. Hou L, Wu P (2019b) Two-dimensional correlation infrared spectroscopy of heat-induced esterification of cellulose with 1,2,3,4-butanetetracarboxylic acid in the presence of sodium hypophosphite. Cellulose 26(4): 2759-2769.
15. Hubbe M A, Bowden C (2009) Handmade paper: a review of its history, craft, and science. BioResources 4(4): 1736-1792.
16. Inagaki T, Siesler H W, Mitsui K, Tsuchikawa S (2010) Difference of the Crystal Structure of Cellulose in Wood after Hydrothermal and Aging Degradation: a NIR Spectroscopy and XRD Study. Biomacromolecules 11(9): 2300-2305.
17. Jeong M-J, Kang K-Y, Bacher M, Kim H-J, Jo B-M, Potthast A (2014) Deterioration of ancient cellulose paper, Hanji: evaluation of paper permanence. Cellulose 21(6): 4621-4632.
18. Jeong M J, Bogolitsyna A, Jo B M, Kang K Y, Rosenau T, Potthast A (2014) Deterioration of ancient Korean paper (Hanji), treated with beeswax: A mechanistic study. Carbohydrate Polymers 101: 1249-1254.
19. Kocar D, Pedersoli J L, Strlic M, Kolar J, Rychly J, Matisova-Rychla L (2004) Chemiluminescence from paper II. The effect of sample crystallinity, morphology and size. Polymer Degradation and Stability 86(2): 269-274.
20. Lin Q, Huang Y, Yu W (2020) An in-depth study of molecular and supramolecular structures of bamboo cellulose upon heat treatment. Carbohydrate Polymers 241: 116412.
21. Liu X Y, Timar M C, Varodi A M, Sawyer G (2017) An investigation of accelerated temperature-induced ageing of four wood species: Colour and FTIR. Wood Science and Technology 51(2): 357-378.
22. Lojewska J, Lubanska A, Miskowiec P, Lojewski T, Proniewicz L M (2006) FTIR in situ transmission studies on the kinetics of paper degradation via hydrolytic and oxidative reaction paths. Applied

Physics A: Materials Science & Process 83(4): 597-603.

23. Lojewska J, Miskowiec P, Lojewski T, Proniewicz L M (2005) Cellulose oxidative and hydrolytic degradation: in situ FTIR approach. Polymer Degradation and Stability 88(3): 512-520.
24. Lojewski T, Miskowiec P, Missori M, Lubanska A, Proniewicz L M, Lojewska J (2010) FTIR and UV/vis as methods for evaluation of oxidative degradation of model paper: DFT approach for carbonyl vibrations. Carbohydrate Polymers. 82(2): 370-375.
25. Luo Y, Chen J, Yang C, Huang Y (2019) Analyzing ancient Chinese handmade Lajian paper exhibiting an orange-red color. Heritage Science 7(1): 1-8.
26. Luo Y, Cigic I K, Wei Q, Strlic M (2021) Characterisation and durability of contemporary unsized Xuan paper. Cellulose 28(2): 1011-1023.
27. Mallamace D, Vasi S, Missori M, Mallamace F, Corsaro C (2018) NMR investigation of degradation processes of ancient and modern paper at different hydration levels. Frontiers of Physics 13(1): 138202.
28. Moran S D, Woys A M, Buchanan L E, Bixby E, Decatur S M, Zanni M T (2012) Two-dimensional IR spectroscopy and segmental C-13 labeling reveals the domain structure of human gamma D-crystallin amyloid fibrils. Proceedings of the National Academy of Sciences of the United States of America 109(9): 3329-3334.
29. Olsson A M, Salmen L (2004) The association of water to cellulose and hemicellulose in paper examined by FTIR spectroscopy. Carbohydrate Research 339(4): 813-818.
30. Park Y, Jin S, Noda I, Jung Y M (2018) Recent progresses in two-dimensional correlation spectroscopy (2D-COS). Journal of Molecular Structure 1168: 1-21.
31. Saito T, Isogai A (2004) TEMPO-mediated oxidation of native cellulose. The effect of oxidation conditions on chemical and crystal structures of the water-insoluble fractions. Biomacromolecules 5(5): 1983-1989.
32. Tang Y, Smith G J, Weston R J, Kong X (2017) Chinese handmade mulberry paper: generation of reactive oxygen species and sensitivity to photodegradation. Journal of Cultural Heritage 28: 82-89.
33. Teodonio L, Missori M, Pawcenis D, Lojewska J, Valle F (2016) Nanoscale analysis of degradation processes of cellulose fibers. Micron 91: 75-81.
34. Toba K, Yamamoto H, Yoshida M (2013) Crystallization of cellulose microfibrils in wood cell wall by repeated dry-and-wet treatment, using X-ray diffraction technique. Cellulose 20(2): 633-643.
35. Wang Y Y, Tian M, Xu H X, Fan P (2014) Influence of moisture on mechanical properties of cellulose insulation paper. International Journal of Modern Physics B 28(7): 1450051.
36. Xing L, Hu C, Zhang W, Guan L, Gu J (2020) Transition of cellulose supramolecular structure during concentrated acid treatment and its implication for cellulose nanocrystal yield. Carbohydrate Polymers 229: 115539.
37. Yang H, Gong M, Hu J, Liu B, Chen Y, Xiao J, Chen H (2020) Cellulose Pyrolysis Mechanism Based on Functional Group Evolutions by Two-Dimensional Perturbation Correlation Infrared Spectroscopy.

Energy & Fuels 34(3): 3412-3421.

38. Yang J, Lu X, Yao X, Li Y, Yang Y, Zhou Q, Zhang S (2019) Inhibiting degradation of cellulose dissolved in ionic liquids via amino acids. Green Chemistry 21(10): 2777-2787.
39. Yonenobu H, Tsuchikawa S, Sato K (2009) Near-infrared spectroscopic analysis of aging degradation in antique washi paper using a deuterium exchange method. Vibrational Spectroscopy 51(1): 100-104.
40. Zieba-Palus J, Weselucha-Birczynska A, Trzcinska B, Kowalski R, Moskal P (2017) Analysis of degraded papers by infrared and Raman spectroscopy for forensic purposes. Journal of Molecular Structure 1140: 154-162.

Figures

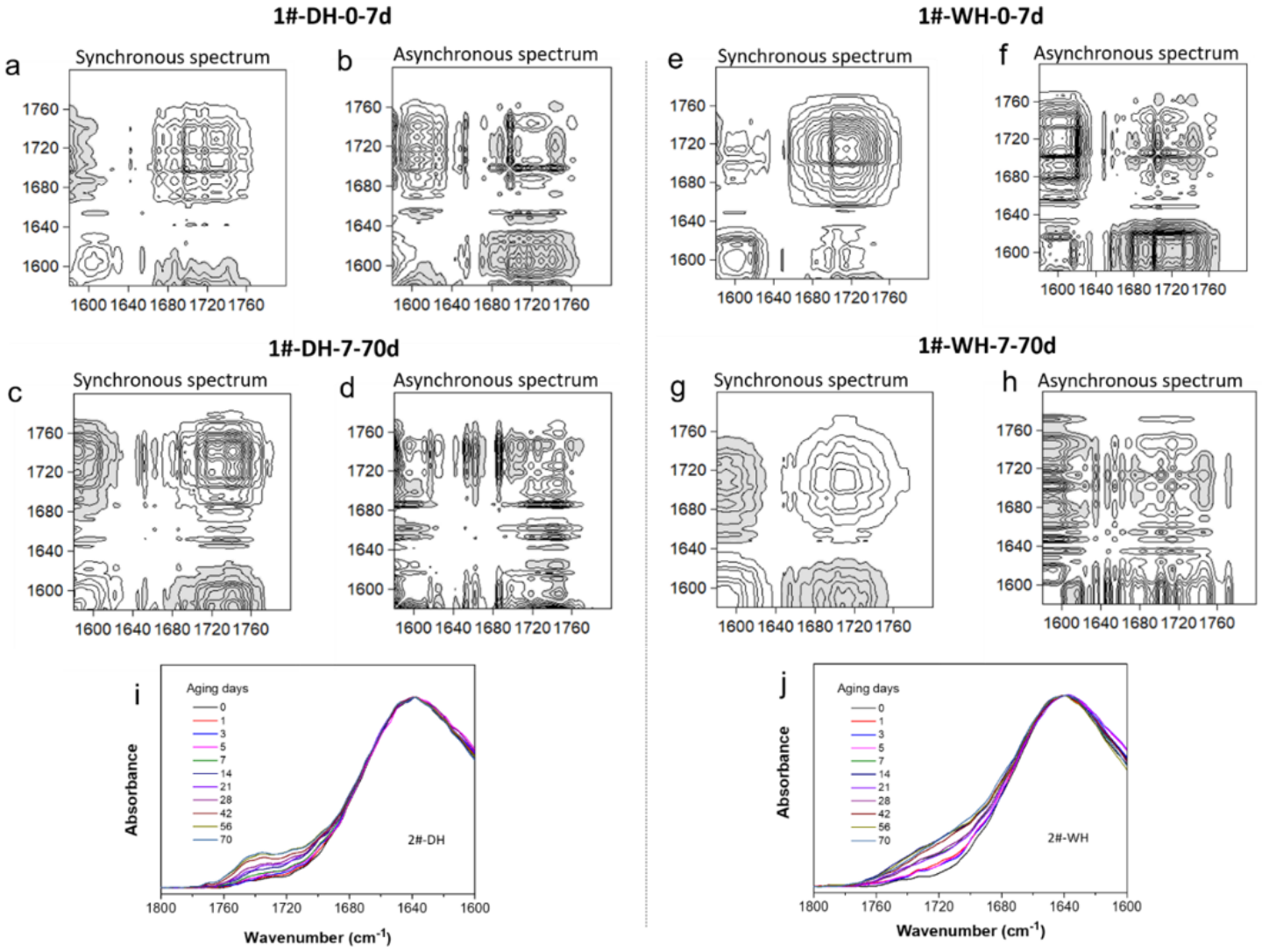

Figure 1

Synchronous and asynchronous 2D-COS (a-h) and FTIR (I and j) of 1# handmade paper in 1800-1580 cm-1 region. The dry-heat and wet-heat treatment time range of 0-7d and 7-70d.

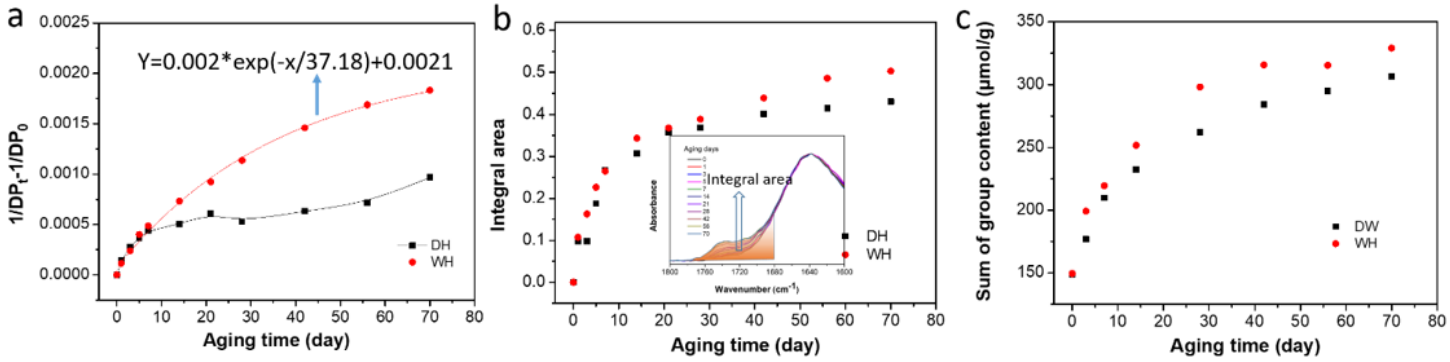

Figure 2

(a) 1/DPt-1/DP0 vs aging time of the four papers at DH and WH condition. (b) Infrared spectral area vs aging time of the four papers at DH and WH condition. (c) The sum of reducing carbonyl and carboxyl content in DH and WH aging process.

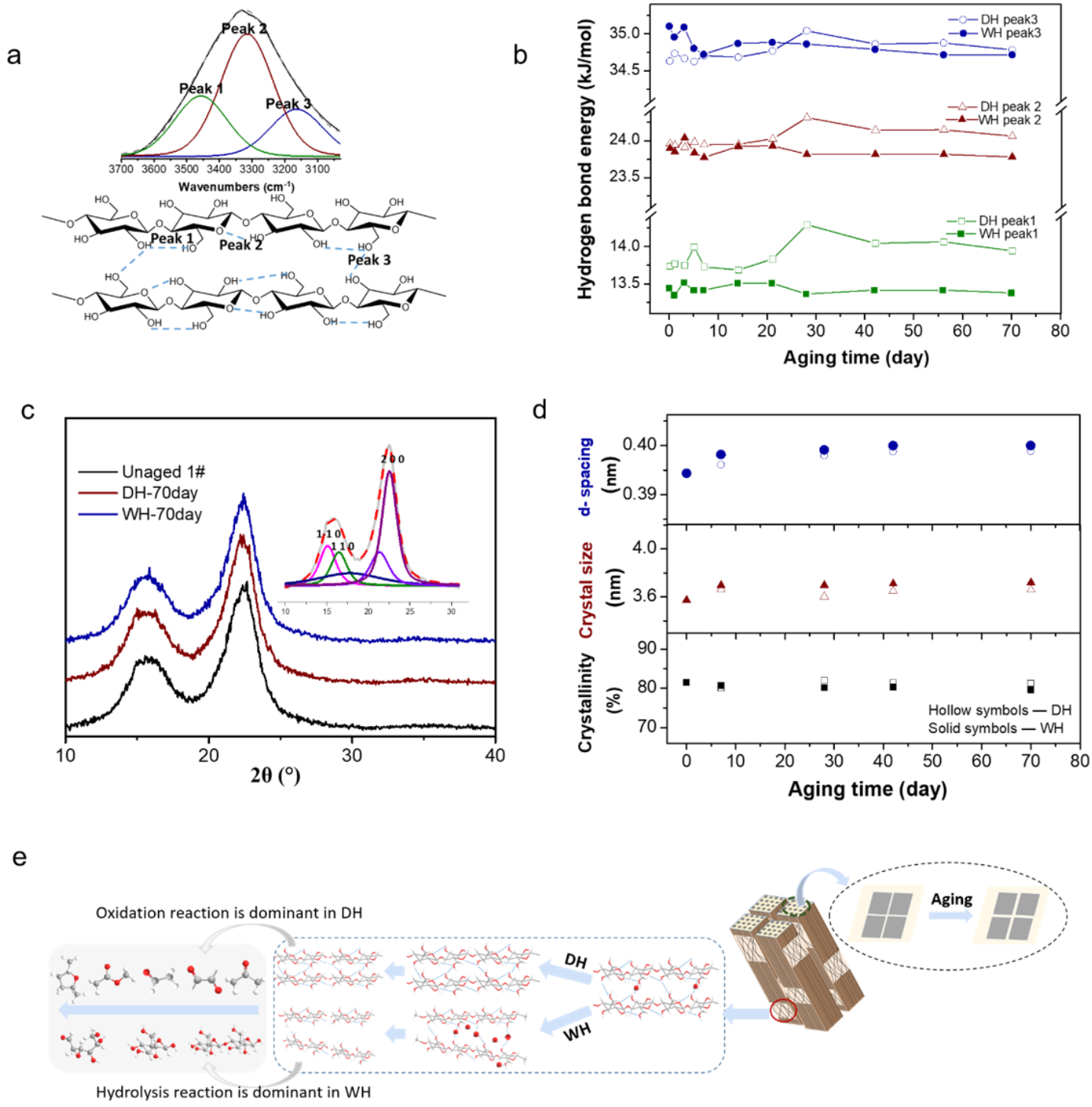

Figure 3

(a) A pattern of H-bonds in the inter- and intrachain structures and peak fitting of FTIR spectrum for unaged 1# handmade paper. (b) The change of hydrogen bond energy for 1# handmade paper in DH and WH aging process. (c) XRD of unaged and 70 days aged 1# handmade paper. (d) The effects of DH and WH aging on crystallinity, crystal size and crystal plane spacing. (e) Schematic pictures indicating the difference of the fine structure of handmade paper in DH and WH aging condition.

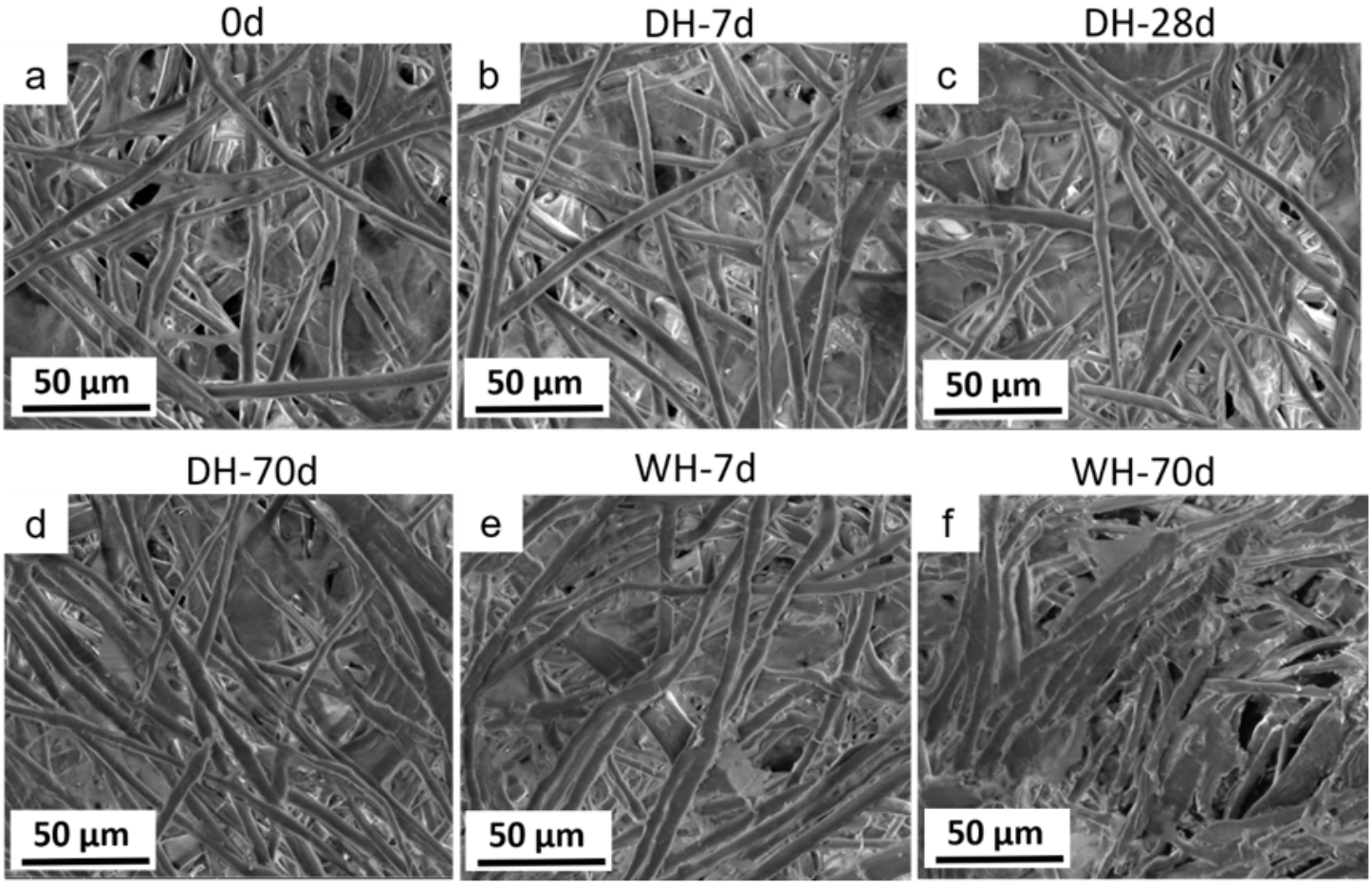

Figure 4

SEM images of unaged 1# handmade paper (a) and 1# with various aging days in DH (b-d) and WH (e-f) condition.

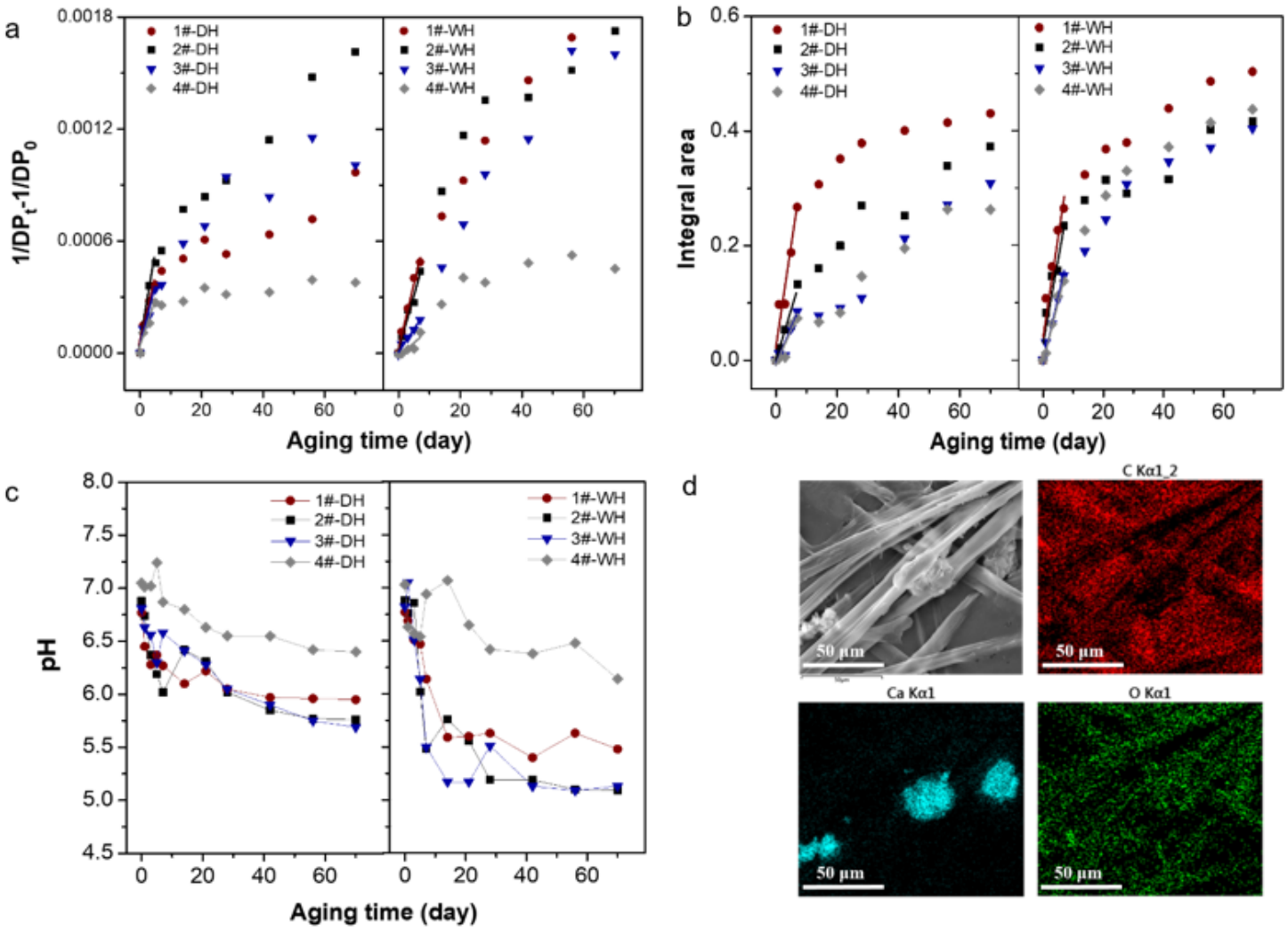

Figure 5

(a-c) Effect of craft and raw materials on number of molecular chain breaks (a), IR integral area (b), and pH (c) of handmade paper in aging process. (d) SEM image and EDS mapping for C, O and Ca of unaged 4# handmade paper.

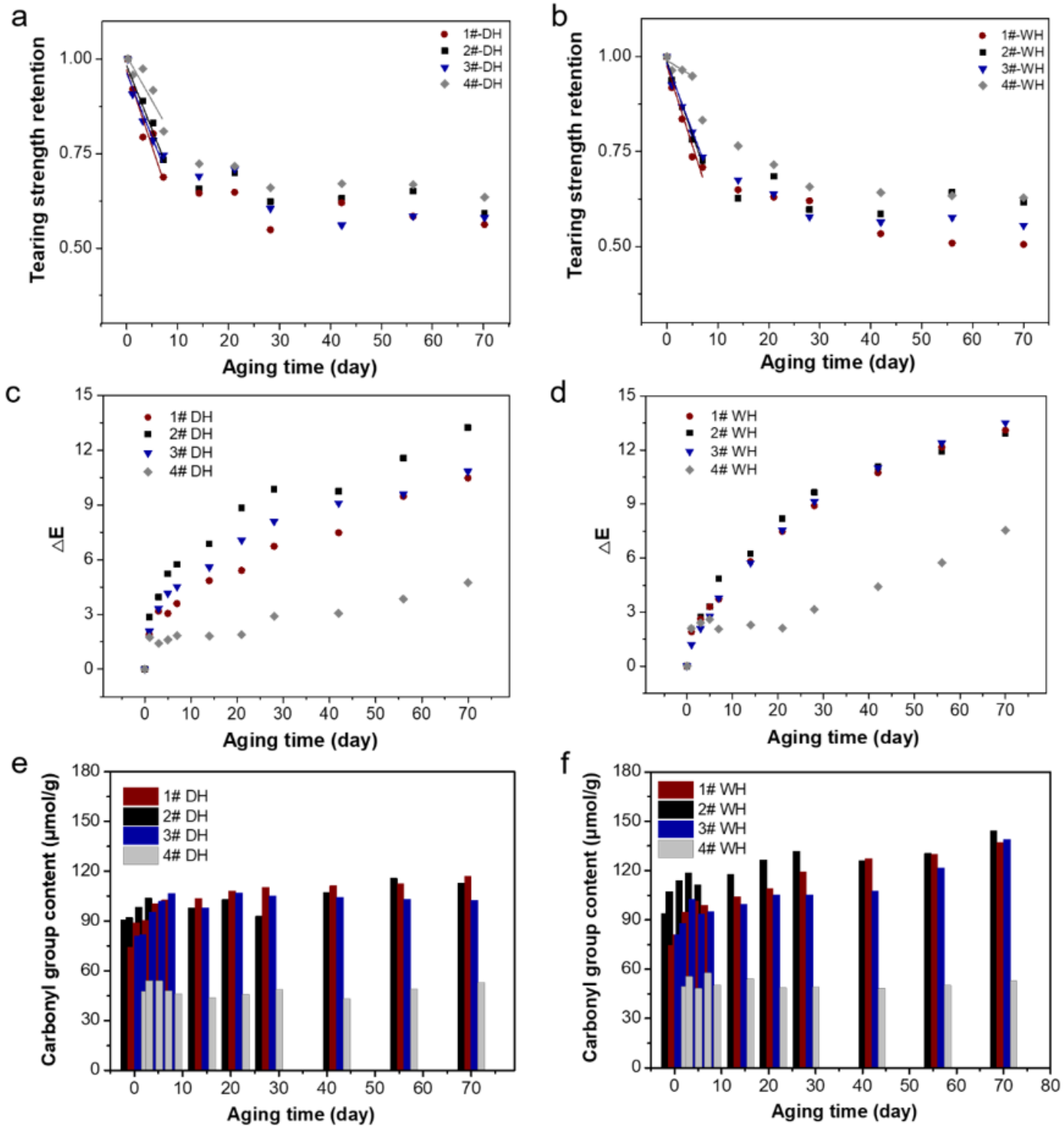

Figure 6

Tearing strength retention (a and b), chromatic aberration (c and d) and carbonyl group content (e and f) of four typical handmade papers at various aging days in DH and WH condition.

Supplementary Files

This is a list of supplementary files associated with this preprint. Click to download.

- Graphicalabstract.docx
- supportinginformation.docx